Check for updates

# Evaluation of the quality of solder joints within silicon solar modules using magnetic field imaging (MFI)

*Kai Kaufmann*, Dominik Lausch, Chia-Mei Lin, Maik Rudolph,, Daniel Hahn, Markus Patzold*

Dr. Kai Kaufmann
Dr. Dominik Lausch
Chia-Mei Lin
Maik Rudolph
Daniel Hahn
Markus Patzold

DENKweit GmbH, Marthastraße 13, 06108 Halle, Germany
E-mail: kai.kaufmann@denkweit.de

Keywords: solar modules, photovoltaics, soldering, reliability, magnetic fields

Solar cells and modules are already a mature technology in mass production. It is critical to optimize and to systematically monitor their performance. The introduction of automated soldering processes and the increasing usage of novel contacting schemes can cause harmful defects, e.g. missing and defective contacts and thus affect the electrical performance of solar modules after production or in field usages. In this work, magnetic field imaging (MFI) is utilized to do a non-destructive, quantitative analysis of the modules in order to investigate the quality of the soldering contacts. In detail the cross connector, interconnector and rear side pads were investigated. The typical in-field observed defects are presented. For the first time the quality of rear side pads under operation were studied in detail. It is shown that (i) directly after production the current conduction takes place not only via the rear pads but also via the press-on contact between bare aluminum and the rear side ribbons., (ii) that an off-centered ribbon on the pad lead to abnormal current distribution and (iii) that single rear side pad break as a function of thermal cycles due to thermo-mechanical stress.

Accepted Article

This article has been accepted for publication and undergone full peer review but has not been through the copyediting, typesetting, pagination and proofreading process, which may lead to differences between this version and the Version of Record. Please cite this article as doi: 10.1002/pssa.202000292.

This article is protected by copyright. All rights reserved

Accepted Article

## Introduction

Solar cells and modules are already a mature technology in mass production. Nevertheless, it is critical to optimize and to systematically monitor their performance and quality. In recent years, the solar industry has been economically successful thanks to high cost savings and increased production capacities.[1] Due to the long service life and high investment costs, the quality of each solar module is of utmost importance for safe investments and guaranteed yields. Trust in brand and quality are more and more becoming a major selling point within PV.

The introduction of automated soldering processes and the increasing usage of novel contacting methods to save costs can cause harmful defects, e.g. missing and defective contacts and thus affect the electrical performance and longevity of solar modules after production or in field usages. Further, the trend towards completely new soldering technologies and solar module schemes i.e. shingled solar cells opens unknown physical and technical challenges.

Established methods such as electroluminescence (EL) or thermography are mostly sensitive to voltage drops at the p-n transition (and effective lifetime according to Fuyuki approximation)[2] or lack spatial resolution, seed and sensitivity for industrial applications respectively.[3] For the analysis of the contacting quality and modern module schemes it is necessary to obtain detailed information about the direction and strength of the electrical currents, ideally in high lateral resolution. A method which can analyze electric currents laterally, contactless and in real-time is the magnetic field imaging (MFI). An approach for measuring in short time over large areas was published recently.[4] The soldering process for module production can be divided in three groups: (i) cross connectors, (ii) interconnector and (iii) rear side pads.

## Experimental

This article is protected by copyright. All rights reserved

Under working conditions or electrical current injection solar modules have a quite typical distribution of the flowing electrical current. An electrical current generates a magnetic field which is described by a fundamental relationship in magnetostatics, the Biot-Savart Law,

$$d\vec{B}(\vec{r}) = \frac{\mu_0}{4\pi} \frac{I d\vec{l}^2 \times \vec{r}}{r^3} \quad (1)$$

where $B$ is the magnetic flux density, $I$ is the current strength $d\ell$ is an element of the conductor, the constant $\mu_0$ is the permeability of free space, and $r$ is the distance between the conductor and the sensor. Under certain conditions such as the presence of a 2D geometry of the electrical conductor, the current density distribution can be calculated from the magnetic field using various approaches. For three-dimensional current distributions, the problem becomes much more complex because the solutions of the inverse magnetic problem are not unique.[5] However, even without knowing the detailed current distribution, it is still possible to trace back to specific defects based on its appearance in the magnetic field measurement. Recently, simulations have been published that quantitatively describe the influence of electrical defects on the magnetic field of solar cells in operation.[6]

The method itself is not new. In 1995 it was shown that 2D current distributions can be investigated by magnetic field measurements.[7] In the following years, several publications with applications in the field of photovoltaics were published. [8,9]

In 2018, an approach was published that uses a line sensor to detect the direction and strength of electric currents accurately and in real time. [4] The sensor utilizes a combination of hall effect and the giant magneto resistance depending on the spatial direction. All three spatial components of the magnetic field are measured simultaneously. The length of this line array is variable; width and height are 30 mm and 1.2 mm respectively. The readout speed can be varied up to 300 Hz. The typical measurement range is 1 µT to several mT which equals current densities in the range of 10 mA/cm² up to several A/cm². The measurements shown here were performed either by DENKweit B-LAB (**Figure 1**) or manually with a hand-held device.

This article is protected by copyright. All rights reserved

Accepted Article

The measurement routine for solar modules is as follows: If flowing currents are guaranteed by light or electric injection the generated magnetic fields are measured by swiping over the solar module. The closer the measurement device the stronger the signal since the magnetic field decreases in a first order approximation quadratically with distance according to equation (1). Therefore, the measurement on the back of the solar module provides higher magnetic field values than the measurement from the glass side, but this is not necessary because the signal strength on the glass side is high enough for recognition of most of the soldering defects. By analyzing and processing the spatial MFI data, one can characterize the different solder joints individually. For the measurements shown in this publication a current of 8A was injected electrically which equals roughly 1000 W/m². To measure only the charge carrier-induced magnetic field, a currentless reference measurement is performed before the actual measurement.

The sensor measures all three components of the magnetic field *Bx, By* and *Bz* simultaneously. For the purpose of the work only *Bx* and *By* are used for interpretation of the measurement data. **Figure 2** shows an example measurement of a 5 busbar half-cell mini module. The current enters the cell through the cross connector on top (in the image), flows though the busbars and then leaves the cell through the busbar on the bottom. According to the left-hand rule, a flowing current in x direction generates a magnetic field in the directions y and z as it is the case with the shown cross-connectors. Accordingly, the current through the busbars (in y-direction) generates a magnetic field in the directions x and z. Since a solar cell is a largely two-dimensional component, the current directions can be derived qualitatively from the components *Bx* and *By*. Currents in z-direction (through the cell) can cause small deviations from this behavior, but these are not considered in this work.

**Cross connector**

This article is protected by copyright. All rights reserved

Accepted Article

In standard solar modules all cells are connected in series. In production, 10 or 12 cells are first connected in series as a string. Usually 6 of these strings are then connected in series by cross-connectors. These cross connectors are only soldered with a single solder point per busbar and therefore represent a weak point.

In **Figure 3a** a section of the lower part of a solar module is shown. The green arrows indicate the direction of the flowing electric current. If the series resistance of the cell has no local inhomogeneities, the current flows evenly distributed through the busbars. In the case that a cross connector was not successfully soldered, no electric current can flow through this solder joint into the associated busbar due to the missing electric contact. The injected (or sun generated) electric current must flow through the remaining busbars. In **Figure 3b and c** the x-component of the magnetic field of a solar cell within a solar module having a broken solder joint is shown in 2D and 3D, respectively. Note that the x-component of the magnetic field is mainly dominated by currents flowing in the direction of the busbars. The broken solder joint is marked with a red cross in **Figure 3a and b**. Consequently, no magnetic field signal can be detected at this position. The current must flow through the remaining busbars leading to an increased signal in the neighboring busbar which is discussed in detail later. Over the whole solar cell area, the busbars are electrically connected with the small grid fingers. Therefore, the current distribution evens out again towards the other side of the solar cell. The overall series resistance Rs of the whole module is increased leading to a slightly reduced module performance. The wave-like structure on the busbar signals visible in **Figure 3c** will be discussed in section “rear side pad soldering”.

In **Figure 4a** a line scan along the position marked with a white dotted line in **Figure 3b** is shown. The intensity of the magnetic field signal is directly linear proportional to the current strength. The current is not evenly distributed to the remaining busbars. Despite the low resistance of the busbars, the distance to the left busbar is higher than for example the busbar neighboring defect. This causes the current to flow increasingly in the adjacent busbar. The peak height at BB1 is 190 µT, at BB2

Accepted Article

This article is protected by copyright. All rights reserved

203 µT, at BB3 233 µT and at BB4 20 µT (not 0 µT since the measurement is performed within the solar cell).

Based on the results and using advanced simulation as presented in [6] one can calculate the loss quantitatively. An estimation of the loss depends on several factors such as irradiation or temperature. For a rough estimation one can assume that the 4 busbars each carry 25% of the current. If one busbar is missing, the other busbars carry the same current, but with a different distribution. Based on the line measurement, a distribution of 30.2%, 32.4% and 37.4% was calculated. Assuming that the series resistance *Rs* increases with $I^2$, the proportion of *Rs* caused by the ribbons increases by 34% for this cell. All other Rs components are of course not taken into account here. This increase might lead to only a small change in power output. Every additional broken busbar, however, leads to a dramatic loss. [10]

By using a simple algorithm, which determines the average magnetic field strength for each busbar, a quality criterion can be derived, which can distinguish between non-contacted busbars and only partially contacted busbars. **Figure 6** shows an example of all cross-connectors (marked with a blue dotted box on the lower part) of a complete solar module including the corresponding magnetic field measurements. Besides completely broken solder joints between the busbar and the cross connectors, the various current differences also reflect the quality of the soldered contacts. The different colors correspond to magnetic flux densities and therefore current strengths in the corresponding busbars. It is obvious that not all contacts show the same solder quality. It is assumed that the influence on the power output is rather low as long as the variations remain in a well-defined range, since single fully disconnected ribbons in three busbar modules lead to a performance drop of 0.85% to 1.5%.[10] The quantification of the influence of these variations is a topic of ongoing research. However, in order to guarantee the module performance, it is necessary to keep the quality of the soldering of the cross connectors as high as possible.

Accepted Article

This article is protected by copyright. All rights reserved

**Interconnectors**

Within a string the individual solar cells are connected in series with tin-coated copper ribbons. With these ribbons the silver grid of the front side of one solar cell is connected to the single silver pads of the back side of the following solar cell. Between the solar cells the connectors are bent to connect from the front side to the back side of the following solar cell.

In order to increase the active area of solar modules the spacing between each solar cell is reduced more and more. Consequently, the bending of the ribbon between the solar cells becomes more and more pronounced. According to Pander et al. [11] a major weak point of these intermediate connectors is this bending and the mechanical tension created by it. One major issue are thermally induced mechanical stresses during temperature cycles. As a result, the electrical connection can break. The production processes must be optimized to reduce the breakage of interconnector caused by these tensions.

**Figure 5** shows a section of a module with two broken interconnectors. The broken interconnectors are marked with a red cross in the schematic in **Figure 5a**. Due to the breakage, no electrical current can flow through this interconnector from one solar cell to the other. **Figure 5b** shows the corresponding x-component of the magnetic field as a mapping at 8 A electrical injection. Due to the fracture of the connectors and the resulting lack of electrical current, the magnetic field is missing at these points. Towards the breakage, the current in the bus bar decreases, because it can flow through the grid fingers into the other bus bars. Away from the breakage, electricity flows through the grid fingers back into the busbar. Again, the fingers lead to an equal distribution of the current in the following solar cell, but the broken connector still leads to an increased series resistance of the current and thus to a reduced performance. If broken connectors occur more frequently in a module type, this indicates systematic problems during production.

In **Figure 6** on the right the solder quality of the connectors of an entire module is shown. Since a current of 8A flows through each cell, in an ideal cell a current of 2A flows through each busbar.

Accepted Article

This article is protected by copyright. All rights reserved

The magnetic flux density in this case is the same for all Busbars. In cells with busbars with reduced conductivity, the current is distributed to the other busbars, the magnetic flux density is different for the busbars in this case. Therefore, the following limits were chosen for the color selection: 0% of the summed magnetic flux density across all busbars for red, 25% of the summed flux density across all busbars for green and 50% (twice the ideal current) of the summed magnetic flux density across all busbars for blue. The color scale is continuous, so also small differences become visible as different shades of green. Although individual broken connectors only lead to a small loss of performance, they are an indication of weaknesses in the production processes of solar modules. Often these occur more frequently over time under operation. Then they can lead to a more significant performance loss. On closer inspection, it is noticeable that the quality of the individual soldered connectors varies slightly. The variations shown here are within the range of normal fluctuations and are always observed. In addition, the measurements were made with a hand-held device, so that there may be uncertainties caused by the operator. Only if the quality of individual connectors deviates too much, this indicates a quality problem of the module. The reason for this can be badly soldered connectors, where the contact between connector and silver paste is not realized properly over the whole surface or simply connectors, which have been soldered slightly offset.

**Rear side pad soldering**

*Detailed analysis*

The back of the solar cell is usually coated entirely with aluminum or, in case of PERC solar cells, with an aluminum/SiN layer stack. The SiN layer contains small openings to enable the contact between the metal and the bulk silicon. To save silver and reduce backside recombination at the poorer interfaces at the silver contacts, usually only 6-8 individually isolated solder pads are used per ribbon. Therefore, there is only a small area where the electric current flows from the front side

Accepted Article

This article is protected by copyright. All rights reserved

to the back side of the solar cell or vice versa (depending on whether the current was injected electrically or by light).

In the case of an energized solar cell, the total current over the cell length changes from the front to the back. If you measure from the back side, the rear side connector is about 200 µm closer to the sensor than the front side connector. The rear connector therefore delivers a higher measurement signal for the same current. This means that the total magnetic flux intensity resulting from the superposition of the magnetic fields of the front and back side changes over the cell length, because it is pronounced by the back side (see **Figure 7a**). This leads to an overall trend of the flux density from one end of the cell to the other. However, this effect might be superimposed by other effects like lateral currents through the cell which can affect the current density of a busbar as well. In order to give a rough estimate of the difference between front and back, the magnetic field of a line conductor can be calculated for different distances. If the distance to the conductor is about 2.5 mm when measuring from the back side (wall thickness of the sensor, distance of the sensor to the backsheet, thickness of the backsheet) the magnetic flux density for a current of 2 A would be 160 µT. If the same current flows about 300 µm further away (200 µm cell thickness, plus 2 times 50 µm to the center of the connector), the flux density is reduced to 143 µT. This difference fits well with the observations in **Figure 7a**.

Due to the rather point-like transition of the current from the front to the back connector, the intensity of the measured magnetic field signal drops abruptly. This might be explained by two possible causes.

1) In the busbar the current has a very distinct direction (in our case in y direction) that causes the magnetic field to have a strong x-component. In the Al layer this restriction is not present, so that the current also distributes laterally. In addition, directly below the bus bar, current flows in the opposite direction to the bus bar, which means that the resulting

Accepted Article

This article is protected by copyright. All rights reserved

magnetic fields partially cancel each other out. The behavior is illustrated in **Figure 7c** for a cell with electrically injected current.

2) Across a cell, the current flows from the front of the cell to the back. The back side is closer to the sensor in the investigations, so that the magnetic generated by the back-side current is slightly pronounced due to the lower distance. As a result, the magnetic field intensity shows a trend across the cell as shown in **Figure 7b**.

These effects lead to the abrupt stepwise decrease in the intensity of the x-component of the magnetic field also shown in **Figure 7a**. The quantitative contribution of each will be topic of a future work. The sum of the current is of course identical, the magnetic flux density, as explained, is not. By analyzing the steps and the intensity difference of the magnetic field, the quality of the soldered backside pads can now be deduced.

The transition of the current from the connector to the cell can be understood even better. Between connector and cell there is a silver pad which is soldered onto the connector. So, the current flows from the connector via the pad into the cell. Here the following effects can be observed. In **Figure 8a** detailed measurement the y-component of the magnetic field of a solar cell in a module is shown. The y-component of the magnetic field is dominated by currents perpendicular to the busbars. There are several remarkable features:

1) It was found that the current flows point-wise from the ribbon into the solder pad, which is also supported by the stepwise reduction in magnetic flux density in **Figure 7c**. This was observed in all cases so far. As a naïve conclusion one can reduce the rear pad size in order to save costs. However, it must be investigated in detail.

2) Some rear side pads do not carry current. It can be assumed that there is no electrical contact anymore. One possible reason is the failure of the contact due to thermal mechanical stress.

This article is protected by copyright. All rights reserved

Accepted Article

Individually failed soldering pads do not lead to a measurable drop in the performance of the solar modules. However, if this occurs more frequently, the series resistance of the solar module is increased and thus its performance is reduced.

3) A positive or negative magnetic field can often be observed around the contact points, to the left and right of the solder point. The red (negative values) and blue colors (positive values) can be attributed to the different direction of the electric currents. These currents are the electric currents flowing within the rear side silver pads. For a pad soldered perfectly in the middle, the current distribution is symmetrical and so is the distribution of the magnetic flux density as shown in **Figure 8b**. It is noticeable that this is not the case for all pads. Some pads are characterized by the presence of only one side or the two sides are not equally pronounced. This can be attributed to the connector being soldered onto the pad with a slight offset as visualized in **Figure 8**. If the connector is soldered on the right side, the current is distributed in the pad by flowing to the left and vice versa (shown in **Figure 8c and Figure 8a**). In conclusion, it is possible to judge how accurately the pad was hit during the soldering process. Basically, this reflects the quality of the soldering process.

*Thermal cycle tests*

It is interesting to note that the solder joints fail more frequently, especially during thermo-mechanical load. In **Figure 9** the solder pads of a solar cell after 100 temperature cycles (TC100) from -40 °C to 85 °C and after 200 cycles (TC200) are compared. As a reference the initial MFI image before TC testing is shown in **Figure 9a**. In this representation, the z-component of the flux density was chosen and the derivative in y-direction was calculated to show the effect more clearly. Initially, the solder joints are barely visible which is explained later in this section. The solder joints of interest are marked with a dotted box. After TC 100 (**Figure 9b**) only the signal of the two back side pads in busbar 2 is missing. The remaining pads vary in quality, but they are still present. The

This article is protected by copyright. All rights reserved

Accepted Article

solder connections in the right busbar are only weakly visible, which indicates a bad electrical contact. After 200 cycles (**Figure 9c**) three rear side pads marked with dotted boxes are missing in the magnetic field measurement. This effect can be observed frequently with MFI. The more thermal cycles a solar module has seen, the more solder pads have failed. Therefore, it can be assumed that the soldering pads break due to the thermally induced stresses caused by the different thermal expansion coefficient of the materials. A similar result is shown in. [12]

In order to systematically investigate this behavior, backside solder pad quality was investigated for different numbers of thermal cycles. After a certain number of thermal cycles, the modules were from the climatic chamber for an intermediate examination. Here, MFI measurements were performed and analyzed the solar module parameters by a sun simulator. **Figure 10** illustrates the presence of solder pads as a function of the thermal cycles performed (TC0 to TC400). For a statistically significant evaluation, 10 mini modules having 240 rear side pads were used. Since the goal was to develop a method capable of meeting production requirements, the values for pad presence was acquired by evaluating the autocorrelation function of the Bx signal along the busbars. The autocorrelation function shows local maxima at periodicities that match a single (or multiples) of the pad distance. Is a pad missing or not visible at all (like it is the case at TC0) the local maxima drop accordingly.

The values in the graph were acquired by a procedure consisting of three steps. First, the autocorrelation function for the Bx signal for each busbar was calculated. Second, the amplitudes for the for the periodicities that match multiples of the pad distance $d_{pad}$ were calculated. Third, these amplitudes were weighted, summed up and averaged over each cell. For summing up the amplitude height for a periodicity of $d_{pads}$ was weighted with 1, for $2*d_{pads}$ with 0.5 and for $3*d_{pads}$ with 0.25. Another reason for choosing this approach is that neighboring missing soldering joints

Accepted Article

This article is protected by copyright. All rights reserved

lead to a bigger decrease in the pad presence value, since it is likely that neighboring defects have a higher impact on module performance.

Following remarkable results were obtained:

1. In **Figure 10a** the presence of present rear side pads as a function of the thermal cycles are shown. Interestingly, directly after the production (TC0) no pads were detected by means of MFI. The reason for this can be seen in **Figure 11**. The reason for this is that directly after production, the electric current is transferred from the rear side solder ribbon into the solar cell over the entire length of the solder ribbon both via the silver/ribbon interface as well as via the aluminum/ribbon interface in between the rear side pads clearly visible in **Figure 11a** (TC0 – black line)In this state it is not possible to examine the individual backside pads. The pressed contact between the solder ribbon and the full surface aluminum backside seems to be good enough for an electrical conduction. However, already after a few thermal cycles the electrical resistance at the interface between the solder ribbon and the aluminum layer increases strongly, so that the current now flows only over the individual solder pads. It is assumed that this is due to the formation of a thin electrically non-conductive aluminum oxide layer. The effect is shown in greater detail in **Figure 11b**. The line graph shows the magnetic flux density *By* along the same busbar after 0, 50, 100 and 400 thermal cycles. For the line plots a constant baseline (minimum value of By in the along the extracted line data) was subtracted to accommodate for a constant background in the magnetic field data. It is clearly visible that the wave-like structure is missing in the beginning but present for 50 or more cycles. The pronunciation of these ripples reaches a limit at 100 cycles. These observations match those of Urban [12], who performed electrical measurements on the backside to determine contact resistances for the press contacts and solder contacts before and after TC tests. Since these observations were made for all modules investigated so far, it can be concluded that a pure press

Accepted Article

This article is protected by copyright. All rights reserved

contact is not sufficient for proper electrical contacting from solder ribbon to cell, which contradicts the result of Dupuis.[13]

2. After 50 cycles nearly all soldered rear side pads are visible except pads which are not successfully soldered during production. As discussed above, the rear side pads can fail due to thermomechanical stresses. Whether this is the case depends strongly on the properties of each individual connection and on the local characteristics of the thermomechanical stresses, which leads to a large scattering for the presence parameter. In sum, however, a clear trend can be observed over several modules. With increasing thermal cycles, the amount of electrical conducting rear side pads decreases as it was also stated by Urban et al.[12]

Single broken rear side pads have a minor influence on the overall performance of the solar module. However, if more than one rear side pad per busbar is broken, the serial resistance goes up.[14] Detailed studies on how many broken rear side pads lead to which loss of performance have not yet been conducted. **Figure 10b** shows, however, the performance loss as a function of thermal cycles for all 10 modules. Here, too, the trend is a drop in performance with increasing number of thermal cycles. It should be noted, however, that additional effects do of course influence performance losses and that the loss cannot be clearly attributed only to the reduced number of rear contacts.

**Summary**

Within this publication the solder joints of standard silicon solar modules were investigated using the magnetic field imaging method. It was shown:

*Cross connector*

Cross-connectors are soldered through a single soldering point. Typical defects are missing solder joints or broken connectors. Both effects have been characterized using MFI. The MFI data allows

Accepted Article

This article is protected by copyright. All rights reserved

a quantitative evaluation of the currents flowing through the connectors, both at cell and module level.

*Interconnector*

Between each solar cell, the ribbon is bend in order to connect from the front side to the back side. These bending can break during production or thermo-mechanical stress in the field. One example of a broken interconnector using MFI is shown and discussed including a full module analysis.

*Rear side soldering*

It has been shown that directly after lamination, current also flows from the ribbon into the cell via the non-soldered areas hence the press on contact between ribbon and aluminum. However, already after few cycles it is assumed that a small AlOx layer is formed leading to a high resistivity at these press on contacts. Therefore, the current flows only from the solder ribbon into the solar cell via the soldered rear side pads. Consequently, a bare aluminum/solder ribbon press on contact is not sufficient for production of solar modules.

During the production processes, the solder ribbons often lie off-centered on the pad. The influence of this offset on the current distribution was investigated with MFI. It could be shown that the current in the pad propagates differently depending on the decentration before it flows into the solar cell. The lateral flowing currents in the pad generate a significant signal in the *By* component of the magnetic field. This opens the possibility to investigate the quality of the ribbon placement in production.

After module production, most backside pads carry electrical current. The quality of the electrical connection varies depending on the quality of the soldering process. It has been shown that these backside connections fail more and more during TC tests. This can be attributed to thermal stress caused by different expansion coefficients of the materials, which occur during the heating and cooling phases.

Accepted Article

This article is protected by copyright. All rights reserved

It could be shown that MFI allows to characterize electrical connections in solar modules in a new detailed way. MFI is an additional method that allows new insights into how the electric current propagates in the module and what influence electric soldering defects have on it. This enables better monitoring and controlling of soldering processes, used materials and parameters and thus improves module quality and reliability.

The exact quantitative influence of various contact defects on the module performance is still unclear. In addition, the introduction of new technologies such as multiwire or shingled modules is again raising new questions in the area of reliable contacting.

References

[1] A. Jäger-Waldau, PV Status Report 2019, EUR 29938 EN. Publications Office of the European Union, Luxembourg, **2019**.

[2] T. Fuyuki, H. Kondo, T. Yamazaki, Y. Takahashi, Y. Uraoka, *Applied Physics Letters*, **2005**, 86, 262108.

[3] U. Jahn, M. Herz, M. Köntges, D. Parlevliet, M. Paggi, I. Tsanakas, Review on infrared and electroluminescence imaging for PV field applications,International Energy Agency Photovoltaic Power Systems Programme, IEA PVPS Task 13, Subtask 3.3, report IEA-PVPS T13-12, **2018,** International Energy Agency, Paris.

[4] D. Lausch, M. Patzold, M. Rudolph, C.-M. Lin, J. Fröbel, K. Kaufmann, in *Proceedings of the EU-PVSEC*, **2018**, pp. 1060–1064.

[5] E.A. Lima, A. Irimia, J.P. Wikswo, *The Magnetic Inverse Problem. In: The SQUID Handbook (eds J. Clarke and A.I. Braginski)*, Wiley, **2006**

[6] M. Pander, S. Dietrich, R. Meier, M. Ebert, in *Proceedings of the EU-PVSEC*, **2019,** pp. 1589-1597.

Accepted Article

This article is protected by copyright. All rights reserved

[7] B. J. Roth, N. G. Sepulveda, and J. P. Wikswo, *J. Appl. Phys*., **1998**, vol. 65, no. 1, pp. 361–372.

[8] R. Buchwald, S. Köstner, F. Dreckschmidt, H. J. Möller, *Solid State Phenomena*, **2008**, 178–179, 331–340.

[9] J. Beyer, H. Matz, D. Drung, T. Schurig, *Appl. Phys. Lett.*, **1999**, 74, 2863–2865.

[10] E. Annigoni, A. Virtuani, J. Levrat, A. Faes, F. Sculati, M. M.Despeisse, C. Ballif, *Progress in Photovoltaics: Research and Applications*, **2019**, 27, 5, 424-432.

[11] M. Pander, S. Dietrich, R. Meier, M. Ebert, M., *Proceedings of the EU-PVSEC*, **2016**, 1589-1597.

[12] T. Urban, M. Heimann, A. Schmid, A. Mette, J. Heitmann, *Energy Procedia*, **2015**, 77, 420–427.

[13] J. Dupuis, E. Saint-Sernin, K. Bamberg, R. Einhaus, E. Pilat, A. Vachez, D. Bussery, *Proceedings of the EUPVSEC*, **2010.**

[14] M. Heimann, R. Bakowskie, M. Köhler, J. Hirsch, M. Junghänel, A. Hussack, S. Sachert, *Energy Procedia*, **2014**, 55, 456-463.

Accepted Article

This article is protected by copyright. All rights reserved

Accepted Article

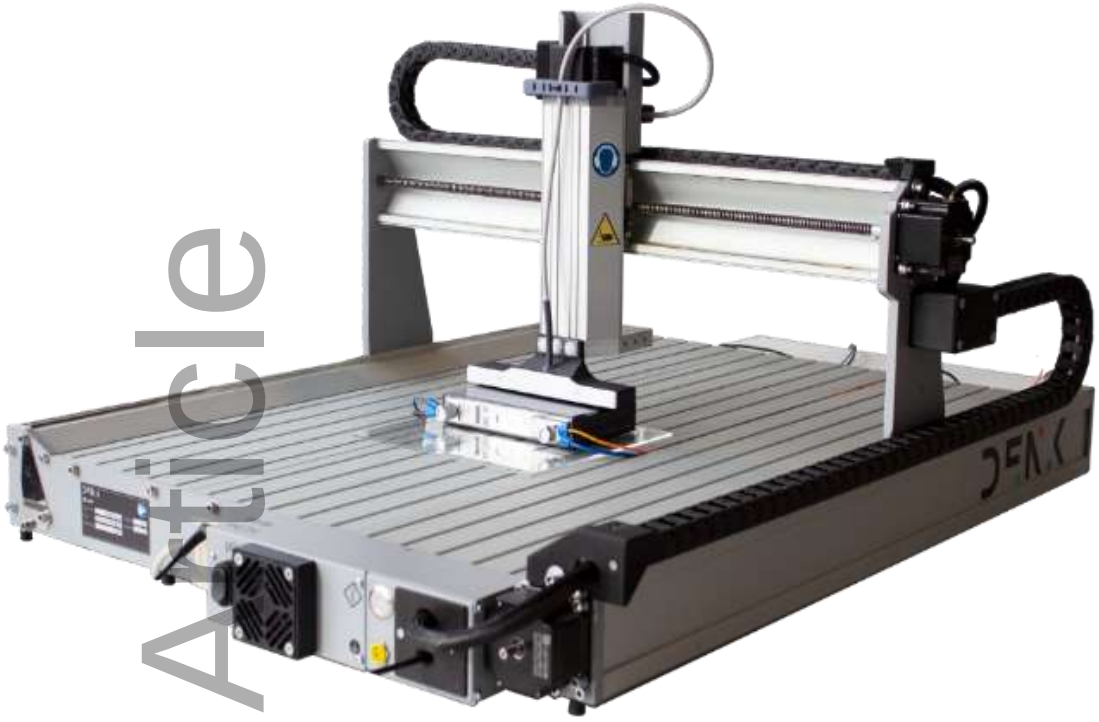

**Figure 1.** DENKweit B-Lab MFI instrument for magnetic field imaging.

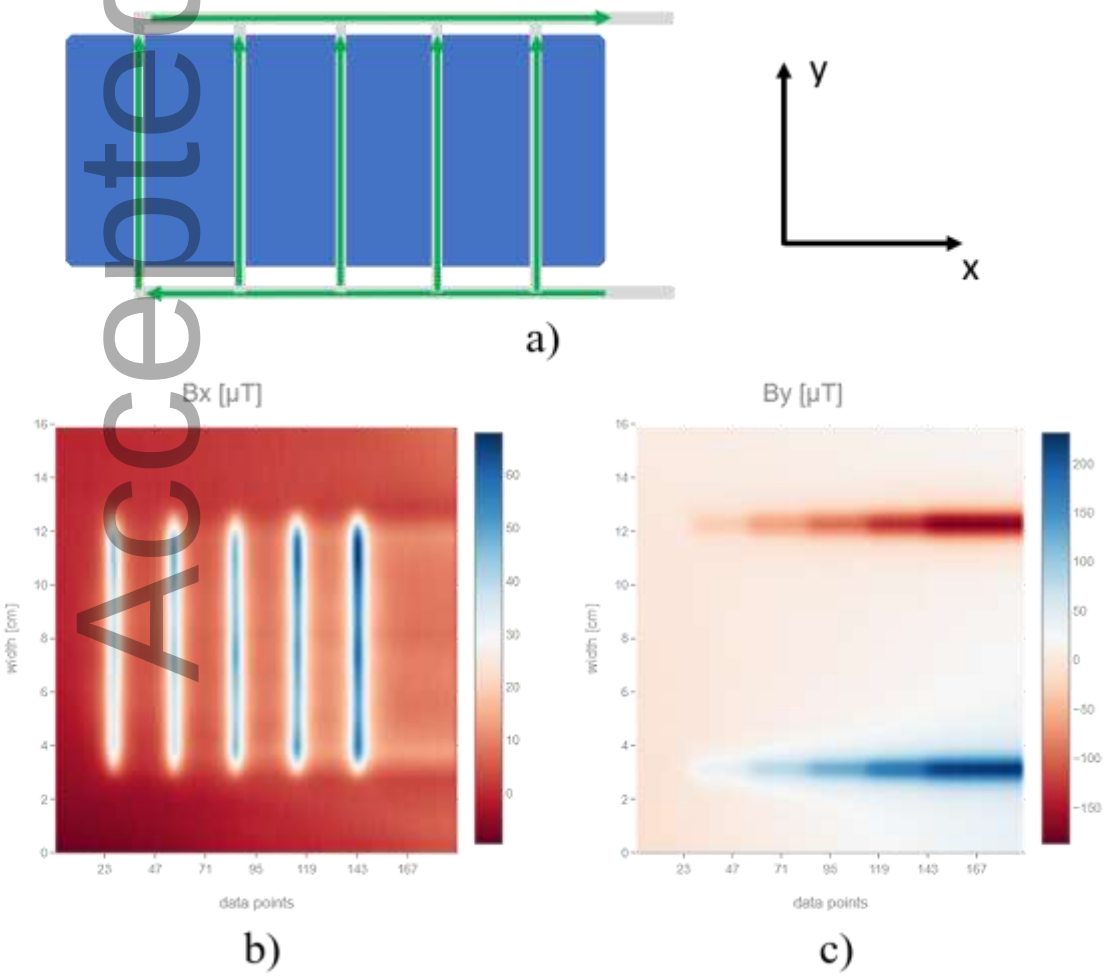


This article is protected by copyright. All rights reserved

**Figure 1**. (a) Illustration of a half cell with cross connectors on both sides The green arrows depict the flowing current. b) *Bx* component of the magnetic flux density. The busbars are visible, but not the cross connectors, because current in x direction does not cause a magnetic field in x direction. c) *By* component of the magnetic flux density. Th busbars are not visible accordingly.

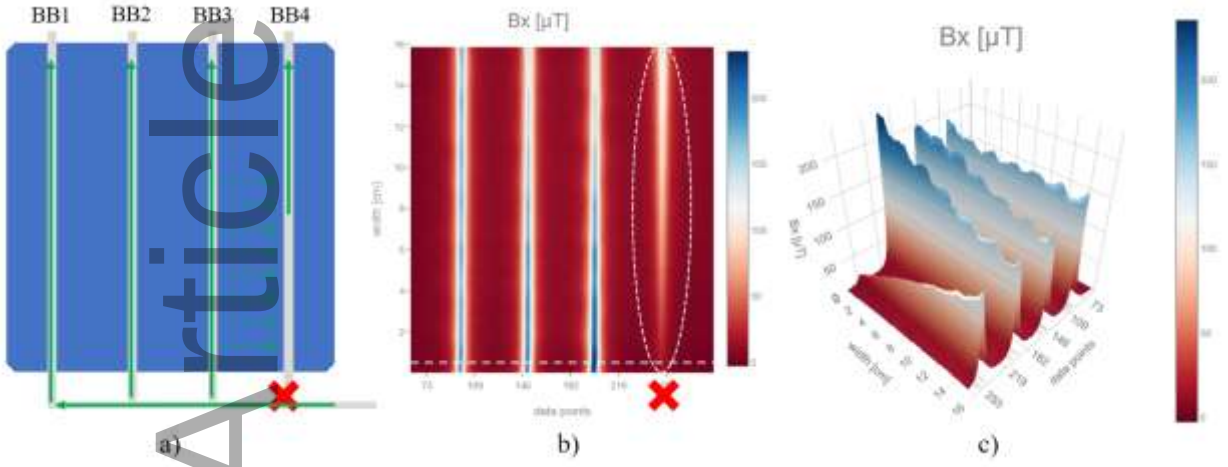


**Figure 3.** (a) Illustration of a solar cell including a cross connector. the green arrows schematically illustrate the directions of current flow under electrical injection. (b) Magnetic field measurement (x-component of the magnetic flux density) of a cell within a solar module. At the red cross the solder joint of the cross connector is defective. (c) 3D image of the same measurement. Due to the broken cross connector a higher current is flowing through working busbars, especially the neighboring busbars.

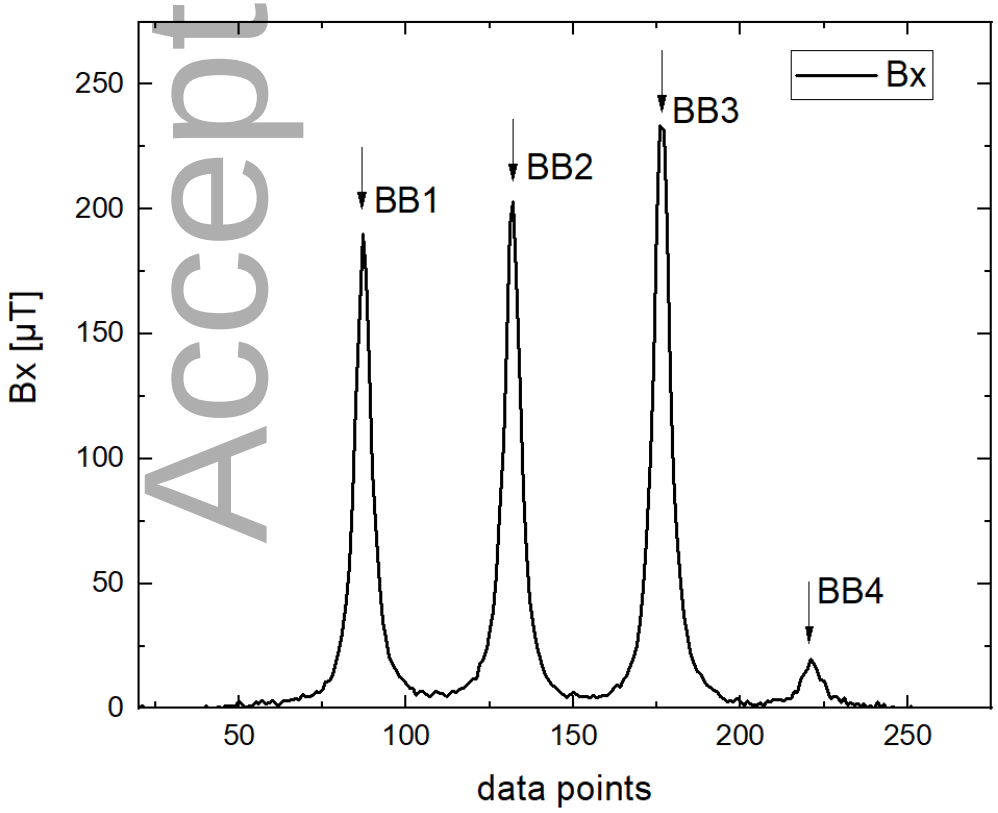


Accepted Article

This article is protected by copyright. All rights reserved

**Figure 4.** x-component of the magnetic flux density along the white dotted line in Figure 3b. The busbars are marked with BB1, BB2, BB3 and BB4 respectively. The defective busbar shows a strongly reduced magnetic field.

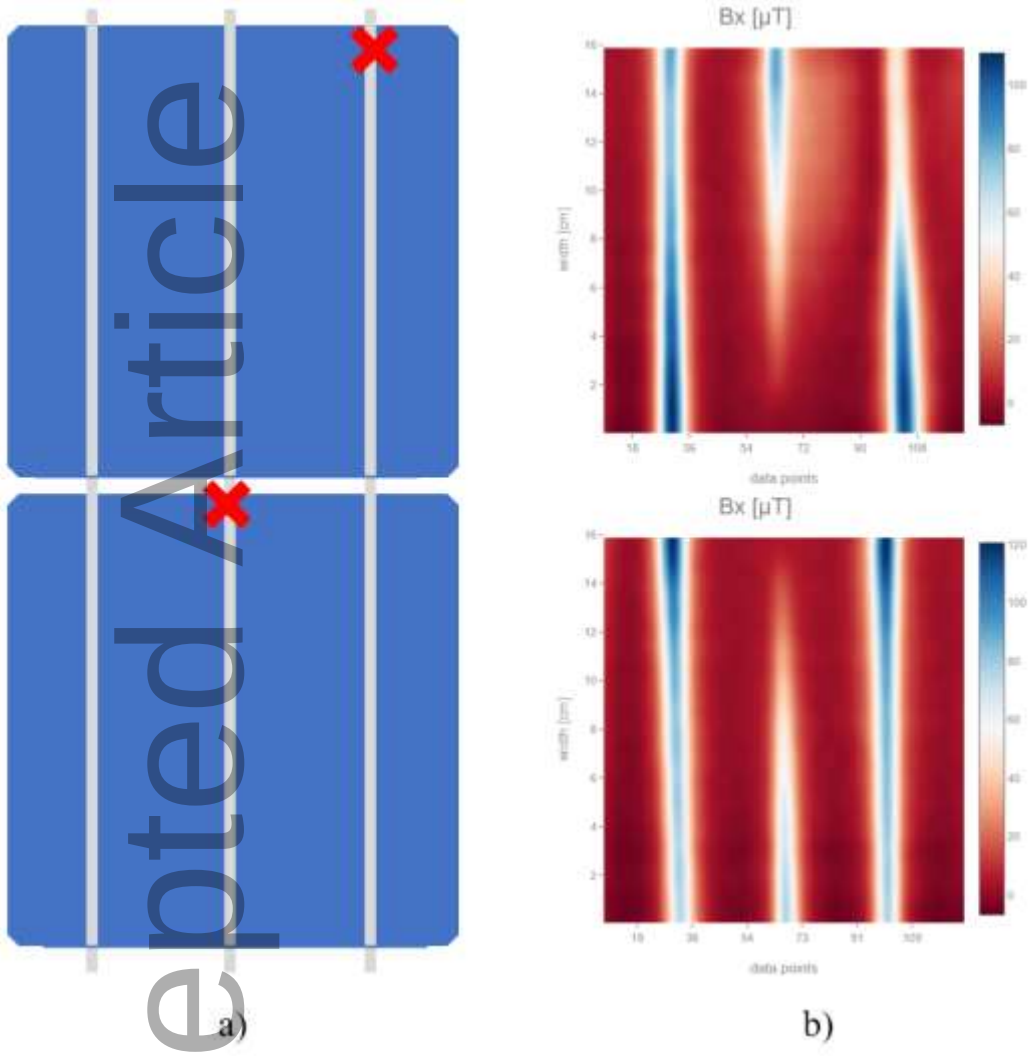


**Figure 5.** (a) Illustration of a section of a solar module. At the red crosses, the interconnectors are broken. (b) Magnetic field measurement (x-component of the magnetic flux density) of two connected solar cells within a solar module. At the failure positions the magnetic field is not present or strongly reduced.

Accepted Article

This article is protected by copyright. All rights reserved

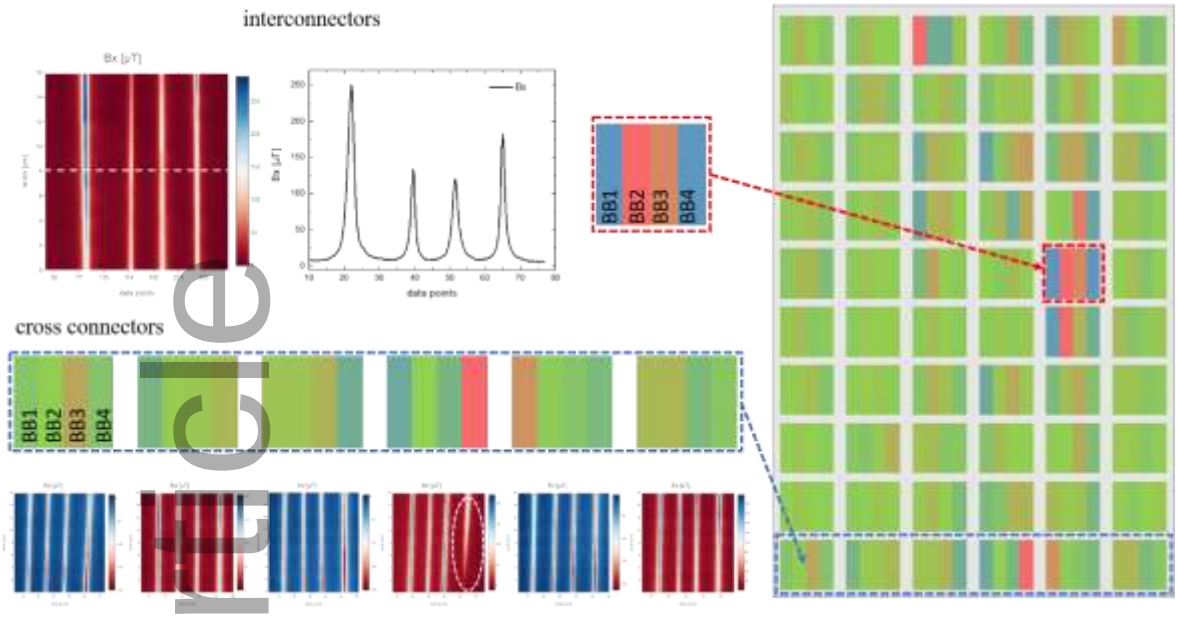


**Figure 6.** Evaluation of the solder quality of a whole solar module for cross and interconnectors. The measurement region for cross connector evaluation is marked with the blue box in the lower part of the module. The region for interconnector evaluation is marked with the red dotted line. The corresponding measurements contain the x-component of the magnetic flux density. The magnetic flux density or current strength respectively is color coded from red (no current) to green (25% of summed flux density) to blue (50% of summed flux density).

Accepted Article

This article is protected by copyright. All rights reserved

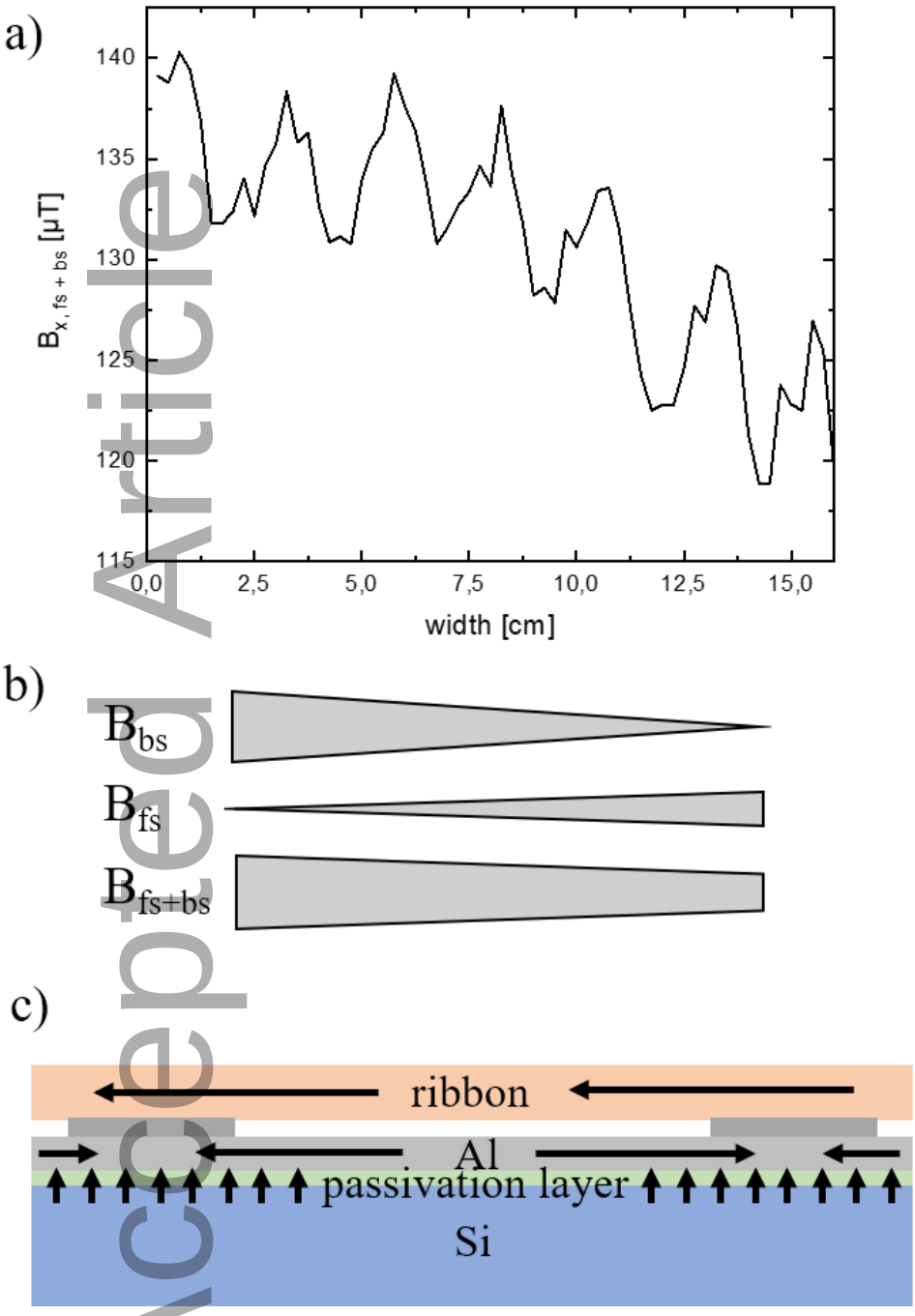


**Figure 7.** a) Flux density along a busbar (measured from rear side). The measured magnetic field is a superposition of front and back, $B_{fs+bs} = B_{bs} + B_{fs}$. Since the rear side is closer to the sensor, this part of the magnetic field is more pronounced. Summing up these to parts leads to a visible trend across the solar cell, according to the sketches in b). The current flow from cell to ribbon in illustrated in c)

Accepted Article

This article is protected by copyright. All rights reserved

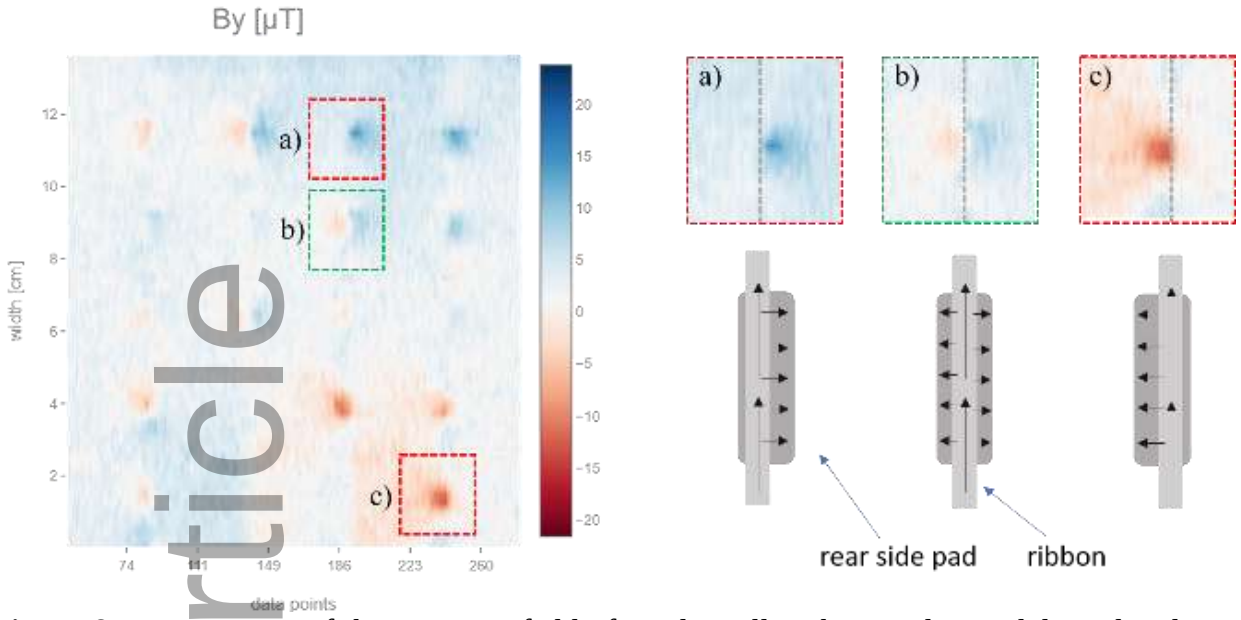


**Figure 8.** y-component of the magnetic field of a solar cell within a solar module under electrical injection. The positive signal (blue) and the negative signal (red) represent currents flowing away from the solder point to the left and to the right respectively. The three extreme cases of solder at the left (a), soldered centered (b) and soldered at the right (c) of the rear side pad are shown.

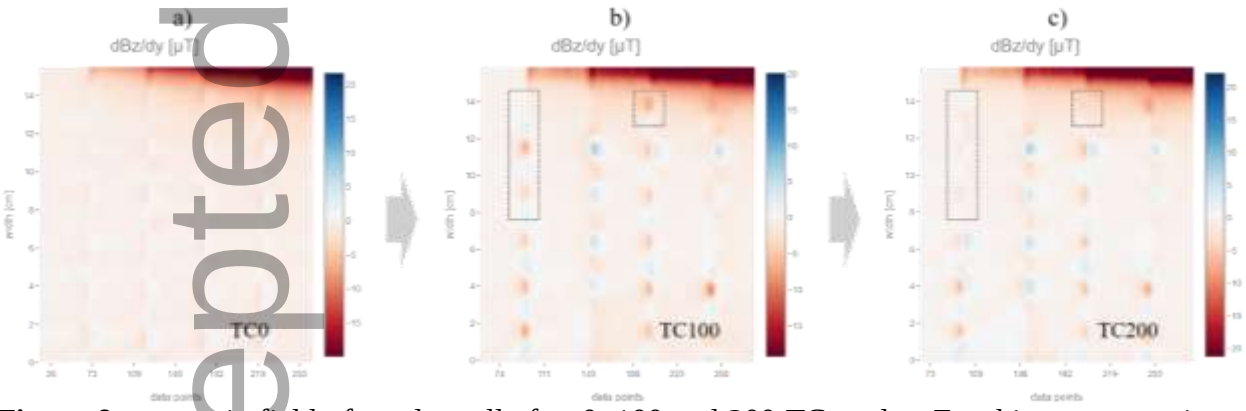


**Figure 9.** magnetic field of a solar cell after 0, 100 and 200 TC cycles. For this representation, the z-component was derived in y-direction. This facilitates the visibility of the solder pads. The soldering joints in the dotted areas vanish or get significantly weaker from TC100 to 200. The strong signal on the top of the cell is caused by the cross connector which connected the individual busbars.

Accepted Article

This article is protected by copyright. All rights reserved

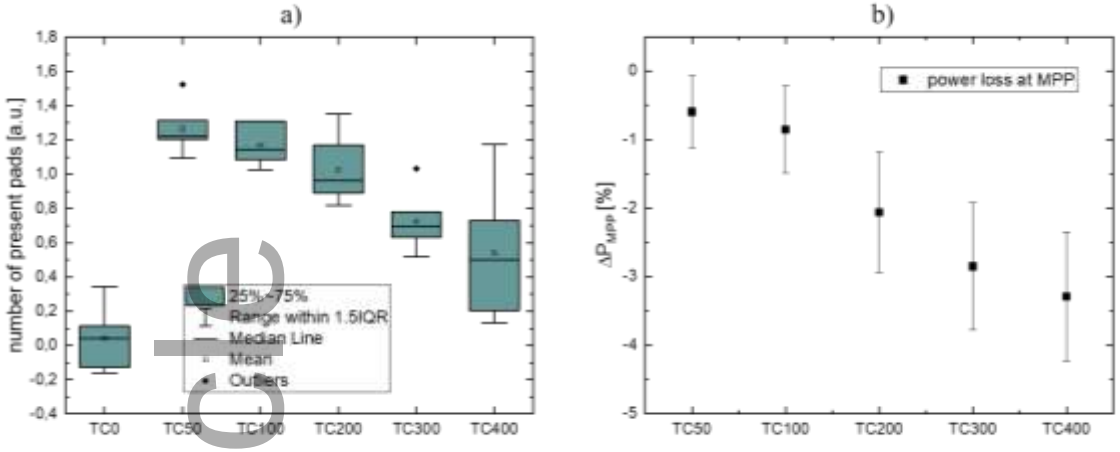


**Figure 10.** Comparison of pad presence a) and performance loss b) for different numbers of TC cycles. pad presence goes down with increasing number of TC cycles. Note, that the presence is low at TC0. Pads are not visible in this state because of present press contacts.

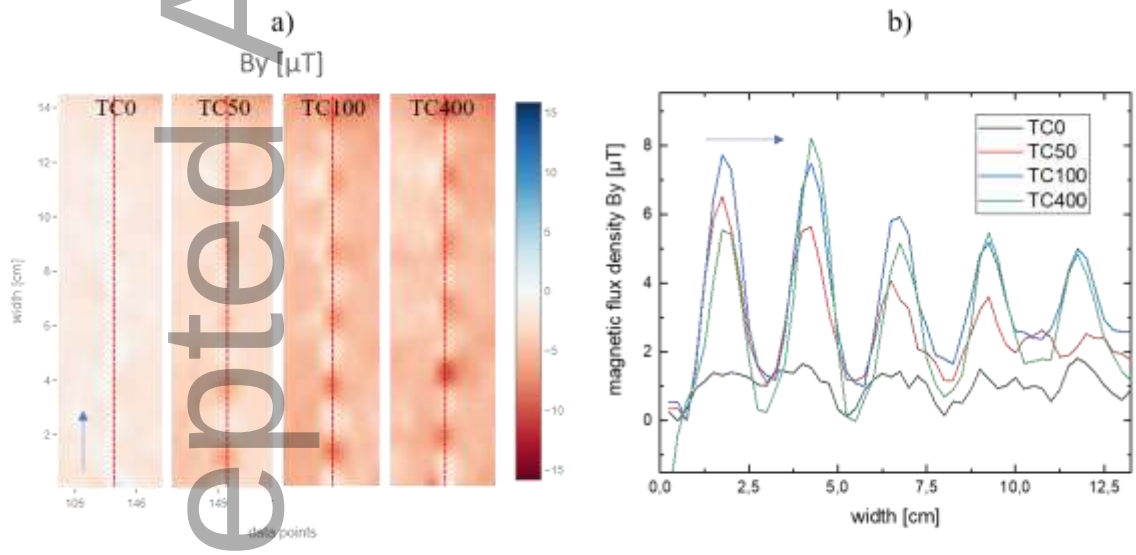


**Figure 11.** a) y-component of one busbar at different numbers of TC cycling, b) line plots of the y-component of the magnetic field along the busbar, the pads are barely visible at TC0 and get mor and more pronounced with increasing numbers of TC cycles. The difference between TC100 and TC400 is, however, rather small.

Accepted Article

This article is protected by copyright. All rights reserved

**Table of contents**

Magnetic field mapping (MFI) is used to assess the contact quality in solar modules. Various critical areas in the solar module are considered, including cross-connectors, interconnectors and the rear side soldering. It is shown that broken connectors and missing solder joints can be detected reliably. Further, the influence of thermal cycling on the presence of solder contacts is discussed.

Keyword: Photovoltaics

*Kai Kaufmann*, Dominik Lausch, Chia-Mei Lin, Maik Rudolph,, Daniel Hahn, Markus Patzold*

**Evaluation of the quality of solder joints within silicon solar modules using magnetic field imaging (MFI)**

Accepted Article

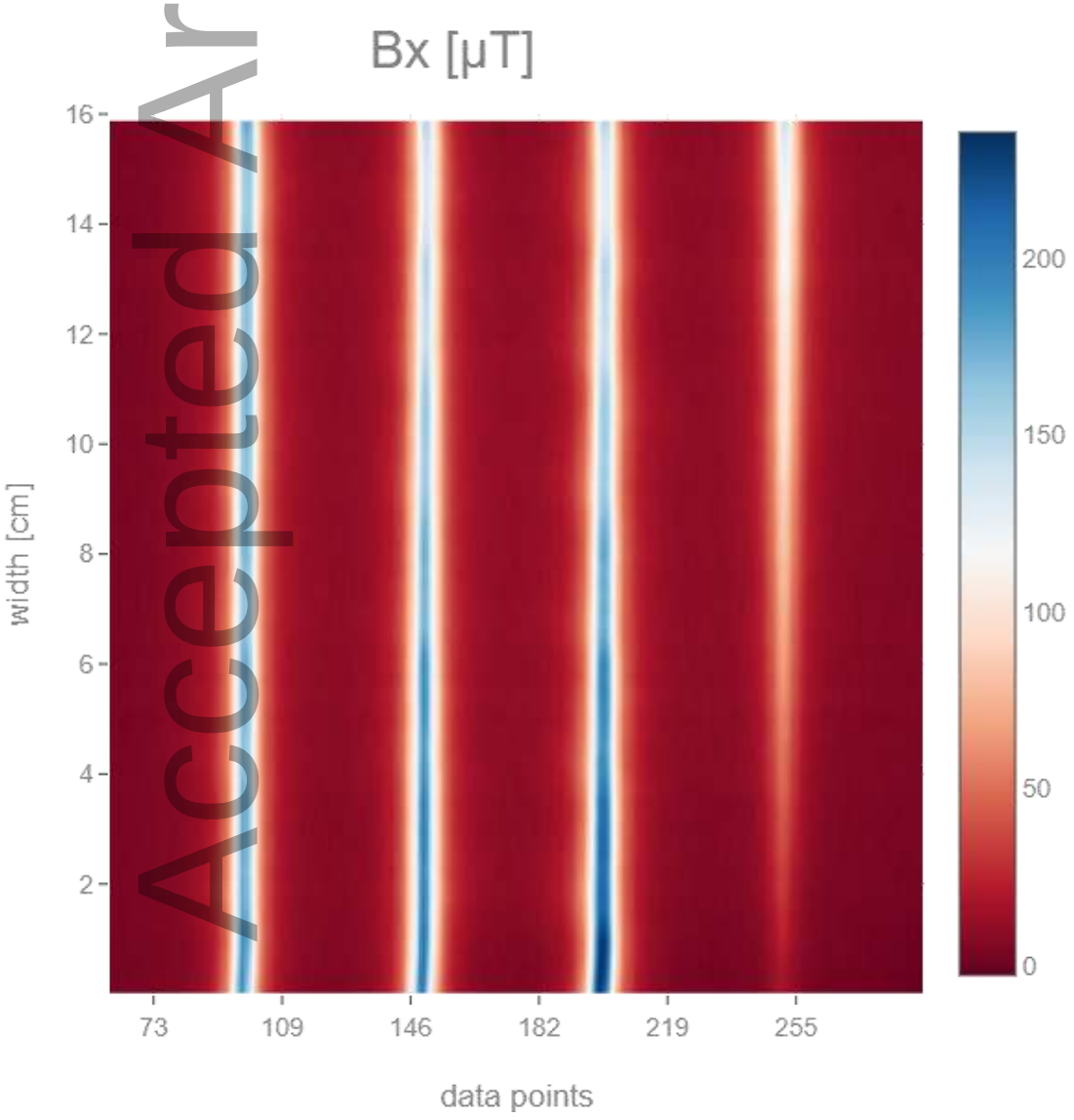


This article is protected by copyright. All rights reserved